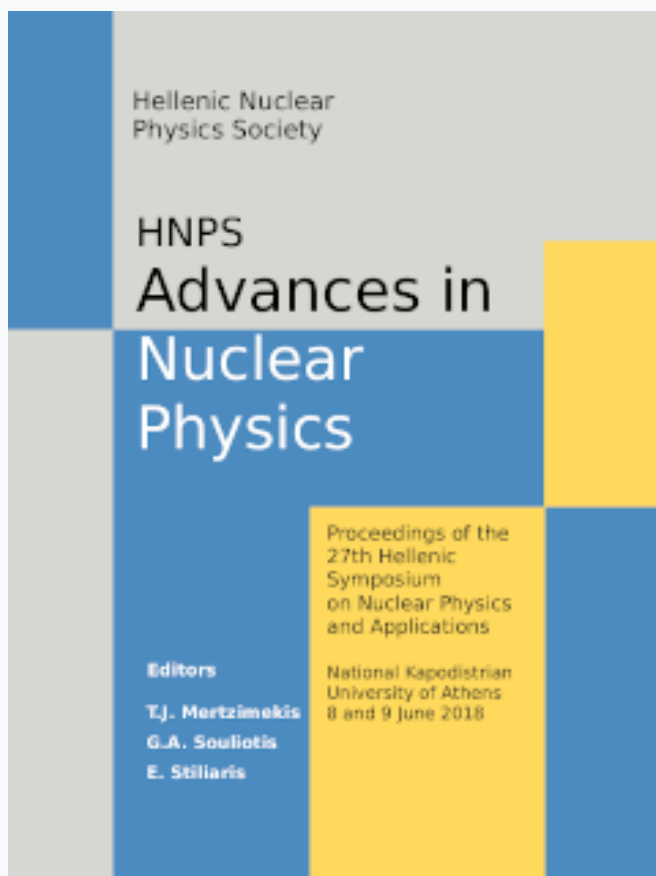


## HNPS Advances in Nuclear Physics

Vol 26 (2018)

HNPS2018



### Measurement of the $^{236}\text{U}(n,f)$ cross-section between 4 and 10 MeV with Micromegas detectors

V. Michalopoulou, M. Diakaki, A. Stamatopoulos, A. Kalamara, M. Kokkoris, A. Lagoyannis, N. Patronis, A. Tsinganis, R. Vlastou

doi: [10.12681/hnps.1815](https://doi.org/10.12681/hnps.1815)

#### To cite this article:

Michalopoulou, V., Diakaki, M., Stamatopoulos, A., Kalamara, A., Kokkoris, M., Lagoyannis, A., Patronis, N., Tsinganis, A., & Vlastou, R. (2019). Measurement of the  $^{236}\text{U}(n,f)$  cross-section between 4 and 10 MeV with Micromegas detectors. *HNPS Advances in Nuclear Physics*, 26, 172–178. <https://doi.org/10.12681/hnps.1815>

# Measurement of the $^{236}\text{U}(\text{n},\text{f})$ cross-section between 4 and 10 MeV with Micromegas detectors

V. Michalopoulou<sup>1,2\*</sup>, M. Diakaki<sup>2</sup>, A. Stamatopoulos<sup>2</sup>, A. Kalamara<sup>2</sup>, M. Kokkoris<sup>2</sup>,  
A. Lagoyiannis<sup>3</sup>, N. Patronis<sup>4</sup>, A. Tsinganis<sup>1</sup>, R. Vlastou<sup>2</sup>

<sup>1</sup> *European Organization of Nuclear Research (CERN), Geneva, Switzerland*

<sup>2</sup> *Department of Physics, National Technical University of Athens, Zografou, Greece*

<sup>3</sup> *National Centre for Scientific Research 'Demokritos', Athens, Greece*

<sup>4</sup> *Department of Physics, University of Ioannina, Ioannina, Greece*

---

**Abstract** In this work, the measurement of the  $^{236}\text{U}(\text{n},\text{f})$  cross-section is presented, in the energy range 4 – 10 MeV, with the use of quasi-monoenergetic neutron beams produced via the  $^2\text{H}(\text{d},\text{n})^3\text{He}$  reaction. The measurements took place at the neutron beam facility of the National Centre for Scientific Research 'Demokritos'. The detection of the fission fragments was achieved with Micromegas detectors placed in a fission chamber, containing both the  $^{236}\text{U}$  targets and the reference samples, namely  $^{238}\text{U}$  and  $^{235}\text{U}$ . The analysis of the experimental data, as well as the first results will be presented.

**Keywords** fission, Micromegas, parasitic neutrons, quasi-monoenergetic neutron beam

---

## INTRODUCTION

The accurate determination of the neutron induced fission cross-section of actinides is of great importance for the design of New Generation Nuclear Reactors IV and Accelerator Driven Systems (ADS). Specifically,  $^{236}\text{U}$  is produced as a by-product of the  $^{235}\text{U}(\text{n},\gamma)$  reaction on the  $^{232}\text{Th}/^{233}\text{U}$  fuel cycle, requiring the knowledge of the corresponding fission cross-section with high accuracy. However, in the energy range between 4 and 10 MeV, the existing experimental datasets [1-5] present discrepancies among them, leading to discrepancies among the latest evaluated libraries [6-8] of up to 8 % (Fig. 1). Therefore, new measurements are necessary for the improvement of the evaluations.

In this scope, the  $^{236}\text{U}(\text{n},\text{f})$  cross-section was measured at the neutron beam facility of the National Centre for Scientific Research "Demokritos" in the energy range 4 - 10 MeV, using Micromegas detectors based on the Microbulk technology.

---

\* Corresponding author, email: veatriki.michalopoulou@cern.ch

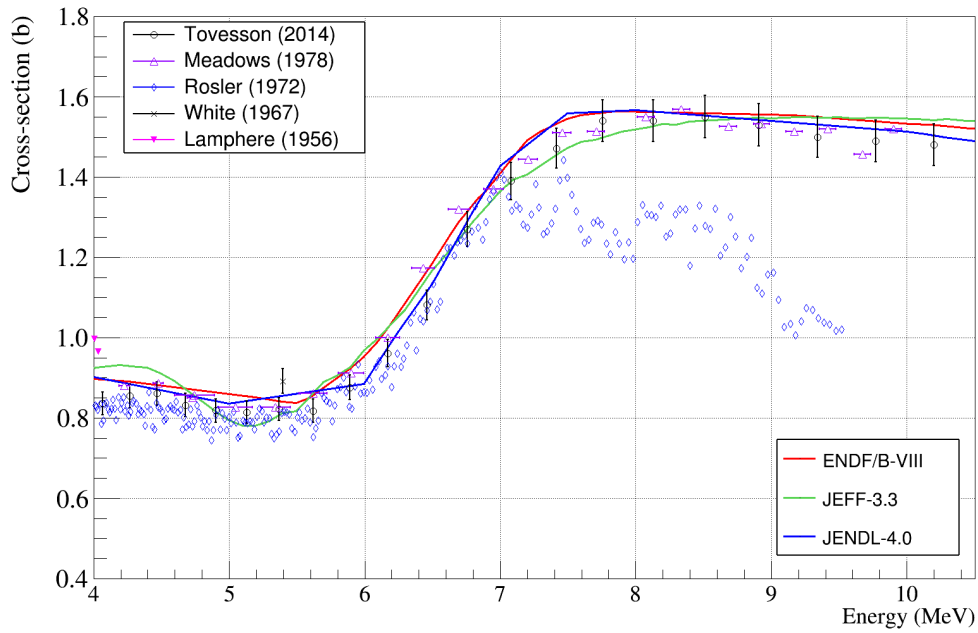


**Fig. 1.** Available datasets in the energy region 4–10 MeV along with major evaluated libraries

## EXPERIMENTAL DETAILS

The experiment was performed at the 5.5 MV Tandem Van de Graaf accelerator of the National Centre for Scientific Research “Demokritos”. The quasi-monoenergetic neutron beams were produced via the  ${}^2\text{H}(d,n){}^3\text{He}$  reaction ( $Q\text{-value} = 3.269\text{ MeV}$ ), by bombarding a deuterium gas target with deuteron beams in the energy range 2 to 7 MeV, while the deuterium pressure was kept nearly constant at 1300 mbar. For each deuteron beam, data were acquired both with and without the deuterium gas in the gas cell, in order to estimate the contribution of parasitic reactions of the deuterons in the beam line and the gas cell materials.

Two  ${}^{236}\text{U}$  targets, two  ${}^{238}\text{U}$  targets and one  ${}^{235}\text{U}$  target were placed inside an aluminium chamber filled with a mixture of 80% Ar and 20%  $\text{CO}_2$  kept at atmospheric pressure. For the detection of the fission fragments each target was coupled with a Micromegas detector, as shown in Fig. 2. A typical spectrum from  ${}^{236}\text{U}$  is shown in Fig. 3.

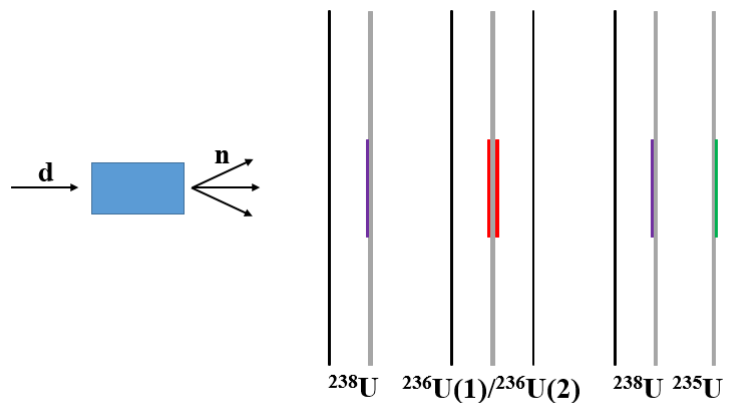


**Fig. 2.** Schematic view of the Micromegas detectors (black) and targets (grey) assembly

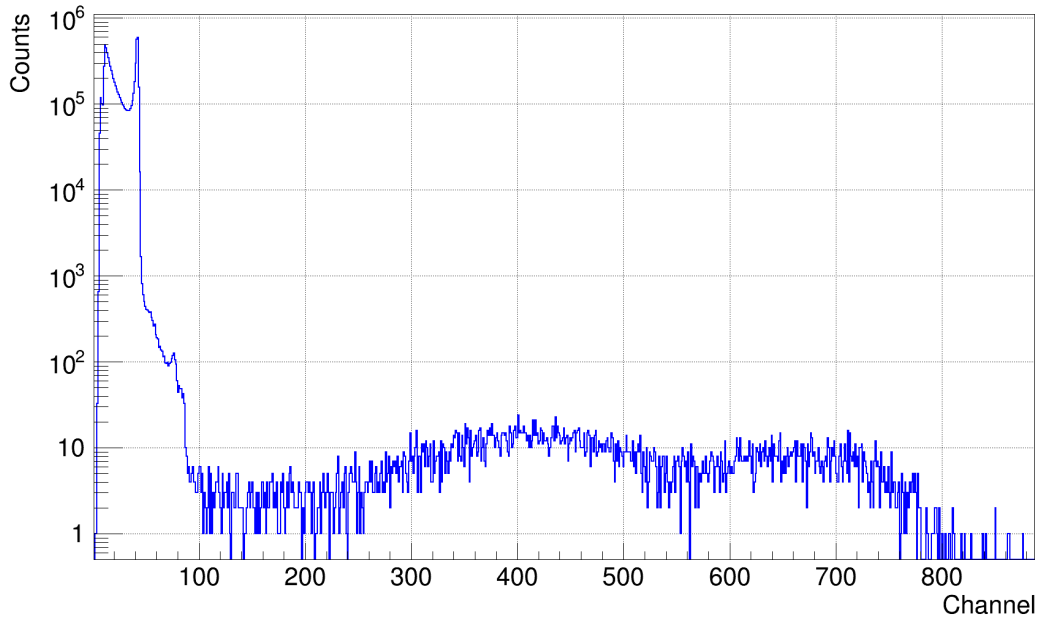


**Fig. 3.** Experimental spectrum from  $^{236}\text{U}(n,f)$  reaction at  $E_n = 10$  MeV

## ANALYSIS

### *Amplitude Threshold*

As seen in Fig. 3 alpha particles, originating from the radioactivity of the actinide targets, are present at the low amplitude region of the experimental spectra (below channel  $\sim 100$ ). As a result, an amplitude threshold is estimated for each target from the beam off spectra, in order to accurately discriminate the fission fragments from the alpha particles. In addition, fission fragments with energy deposition comparable to the energy deposition of the alpha particles are lost under the alpha peak. To recover these lost fission fragments, simulations were carried out with the FLUKA [9] code, using for the mass and kinetic energy of each fragment the distributions generated by the GEF code [10].

### *Parasitic Neutrons*

For the calculation of the  $^{236}\text{U}(n,f)$  cross-section special attention was given to the estimation of the parasitic neutron induced fission reactions in the targets. Specifically, parasitic neutrons are produced from deuteron-induced reactions with the beam line and the structural materials of the gas cell, generating additional parasitic fission fragment counts in the experimental spectra, which need to be subtracted. For each neutron energy, the contribution of this parasitic fission fragment counts, was estimated from experimental spectra with the deuteron gas absent from the gas cell, and subtracted from the total fission fragment counts, after normalizing to the same incident deuteron beam charge. As a result, the clean fission fragment counts  $C(E)$  were estimated for each energy, after correcting for

the parasitic fission fragment counts and for the lost fission fragments below the amplitude threshold.

The contribution from the deuteron break-up reaction, for deuteron energies greater than 4.45 MeV, as well as the neutron scattering in the fission chamber was estimated via Monte Carlo simulations with the MCNP5 code [11], coupled with the NeuSDesc code [12]. However, these simulations underestimate the final source of parasitic neutrons, the neutron scattering in the materials of the experimental area. These low energy neutrons were estimated by applying a low energy neutron flux in order to match the experimental reaction rate of  $^{235}\text{U}(n,f)$  with the reaction rate calculated from the MCNP simulations and the reference cross-section of the  $^{235}\text{U}(n,f)$  reaction, as explained below.

In more detail, the NeuSDesc code coupled with SRIM-2008 [13] provides a neutron source file for MCNP5, taking into account the energy loss as well as the energy and lateral straggling of the deuteron beam in the gas cell materials, the  $^2\text{H}(d,n)^3\text{He}$  differential cross-section and kinematics along with the deuteron break-up in the gas cell. As a result, the neutron energy spectrum and the neutron fluence at the position of each target was estimated from the MCNP5 simulations for each neutron beam energy. The theoretical neutron fluence was used to estimate the theoretical reaction rate for the  $^{238}\text{U}$  targets, normalized to the mass of each target. At this point, a statistical correction factor ( $f_{STAT}$ ) was introduced to normalize the theoretical reaction rate to the experimental reaction rate, obtained from the experimental results. This correction factor, is expected to be the same for all targets, since it is simply a correction factor to match the MCNP5 fluence simulations to the statistics of the experiment, while the relative variations of the flux due to the different distance of the targets from the gas cell are taken into account by the simulations. Still, the theoretical reaction rate of  $^{235}\text{U}(n,f)$ , normalized to the statistics of the experiment for each energy, is underestimated compared to the experimental reaction rate, by a factor varying from 20% to 50%, for different energies. As mentioned above, the MCNP5 simulations underestimate the neutrons scattering in the experimental area, due to the fact that in the simulations the geometry of the whole experimental area was not taken into account, in order to reduce the simulation time. As a result, the small low energy neutron tail from the scattering in the experimental area was not existent in the simulations. While, the absence of these low energy neutrons does not affect the  $^{238}\text{U}$  theoretical reaction rate calculations, due to its low cross-section for neutron energies below the fission threshold, it greatly affects the theoretical calculation of the  $^{235}\text{U}$  theoretical reaction rate. So, a low energy neutron tail, as seen in Fig. 4, is introduced in order to match the  $^{235}\text{U}$  theoretical reaction rate to the experimental one. This low energy neutron flux is used to correct the MCNP5 flux simulations for all targets, after checking that it does not affect the previously calculated theoretical reaction rate for both  $^{238}\text{U}$  targets.

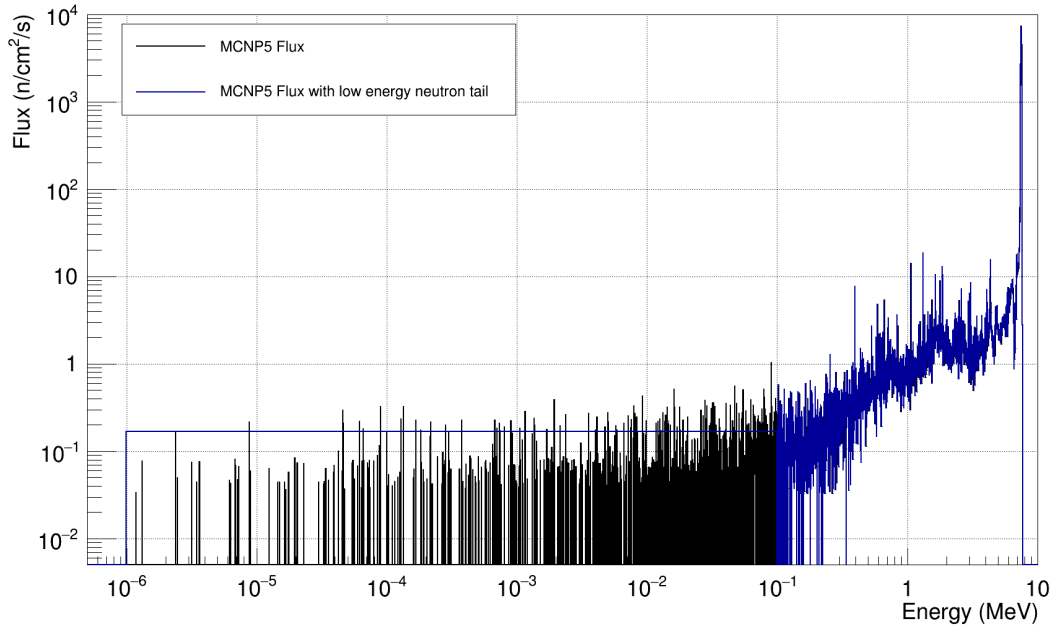


**Fig. 4.** MCNP5 flux results and the low energy neutron flux used for the estimation of the parasitic neutrons at 7.5 MeV energy of the main neutron beam

The flux  $\Phi(E)$  from the MCNP5 simulations, after being corrected for the low energy parasitic tail which was absent in the initial simulations, was used to correct for the parasitic counts coming from the deuteron break-up (for  $E_d > 4.45$ ) and from scattering in the aluminium chamber. Specifically, at each neutron energy the parasitic counts ( $C_{para}(E)$ ) for each target, were calculated from the integrated reaction rate which corresponds to the energies of the parasitic neutrons ( $E_{para}$ ), normalized to the mass of each target ( $N$ ) and to the statistics of the experiment ( $f_{STAT}$ ), via the following expression

$$C_{para}(E) = \frac{\sum_{E_{para}} \Phi(E) \cdot \sigma(E)}{N} \cdot f_{STAT}$$

where  $\sigma$  is the reference cross-section of the target.

### Cross Section

The calculation of the  $^{236}\text{U}(n,f)$  cross section was achieved via the following expression

$$\sigma(E) = \frac{C(E) - C_{para}(E)}{C^{ref}(E) - C_{para}^{ref}} \frac{N^{ref}}{N} \frac{\Phi^{ref}(E)}{\Phi(E)} \sigma^{ref}(E)$$

where

- $C$  are the clean fission fragment counts
- $C_{para}$  are the parasitic counts, estimated via the MCNP5 simulations
- $N$  is the mass of each target, estimated via alpha spectroscopy [14]
- $\Phi$  is the flux which corresponds to the main neutron energy peak, estimated via the MCNP5 simulations
- $\sigma_{ref}$  is the cross-section of the  $^{238}\text{U}(n,f)$  reference reaction

## RESULTS AND DISCUSSION

The preliminary cross-section points with their statistical errors are presented in Fig. 5, along with the previous experimental datasets [1-5] and the latest evaluated libraries [6-8]. The present data are in agreement within errors with the latest data available in EXFOR [1]. In addition, comparing with the latest evaluated libraries, the data are below the evaluations at lower energies and are in agreement with the ENDF/B-VIII.0 [6] and JENDL-4.0 [8] evaluations for the high energy region.

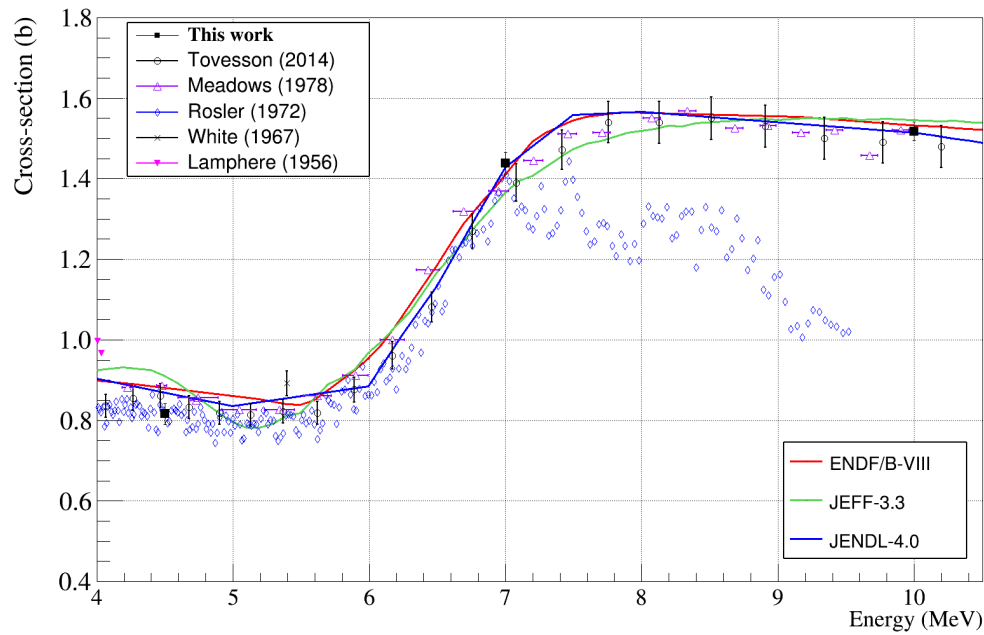


**Fig. 5.** Results of the  $^{236}\text{U}(n,f)$  measurement.

## CONCLUSIONS

In this work, the  $^{236}\text{U}(n,f)$  cross section was measured in the energy range between 4 – 10 MeV, with neutron beams produced via the  $^2\text{H}(d,n)^3\text{He}$  reaction. Special attention was given to the correction of the parasitic neutrons produced from interactions of deuterons with the materials of the beam line and the gas cell, the deuteron break-up as well as the neutron scattering with materials of the experimental setup and the experimental area. With the methodology described above it was made possible, for the first time, to estimate the low energy neutron flux, present in the experimental area and underestimated by the Monte Carlo simulations, using the  $^{235}\text{U}(n,f)$  reference cross-section.

The first cross-section points have been estimated, while the Monte Carlo simulations for the rest of the data is still ongoing. So far, only the statistical errors have been estimated, while for the final cross-section results the systematic error analysis is still in progress.

## AKNOWLEDGEMENTS

This research is implemented through IKY scholarships programme and co-financed by the European Union (European Social Fund - ESF) and Greek national funds through the action entitled Reinforcement of Postdoctoral Researchers, in the framework of the Operational Programme Human Resources Development Program, Education and Lifelong Learning of the National Strategic Reference Framework (NSRF) 2014–2020.

## References

- [1] F. Tovesson et al., Nucl. Sci. and Eng. 179, p. 57 (2014)
- [2] J.W. Meadows, Nucl. Sci. and Eng. 65, p. 171 (1978)
- [3] P.H. White et al., Physics and Chemistry of Fission Conf., Salzburg I, p. 219 (1965)
- [4] H. Rosler et al., Phys. Letters B 38, p. 501 (1972)
- [5] R.W. Lamphere, Phys. Rev. 104, p. 1654 (1956)
- [6] D. A. Brown et al., Nucl. Data Sheets 148, p. 1 (2018)
- [7] JEFF-3.3: Evaluated Data Library 2017, <http://www.oecd-nea.org/dbdata/jeff/jeff33/>
- [8] K. Shibata et al., Nucl. Sci. Tech. 48, p. 1 (2011)
- [9] A. Ferrari et al., <http://cds.cern.ch/record/898301> (2005)
- [10] Schmidt K.H. et al., Nucl. Data Sheets 131, p. 107 (2016)
- [11] Waters L. et al., AIP Conf. Proc. 896, p. 91 (2007)
- [12] Birgersson E. and Loevestam G., Technical Report, EUR 23794 EN (European Commission, 2009)
- [13] J. Ziegler, SRIM 2013, [www.srim.org](http://www.srim.org).
- [14] M. Diakaki et al., Proc. 21<sup>st</sup> HNPS Symposium, p. 81 (2012)